Ocean Systems Engineering, *Vol. 8, No. 1 (2018) 1-20*
DOI: https:// doi.org/10.12989/ose.2018.8.1.001

Evaluation of the new coastal protection scheme at Mamaia Bay in the nearshore of the Black Sea

Dragos M. Niculescu[1,2a] and Eugen V.C. Rusu[*1]

[1]*Department of Mechanical Engineering, University of Galati "Dunarea de Jos", 111 Domneasca Street, Galati, Romania*
[2]*Department of Oceanography, National Institute for Marine Research and Development "Grigore Antipa", 300 Mamaia Blvd., 900581, Constanța, Romania*

(Received August 6, 2017, Revised January 10, 2018, Accepted January 18, 2018)

Abstract. The target area of the proposed study, Mamaia beach, is a narrow stretch of sand barrier island that sits between the Siutghiol Lake and the Black Sea. In the northern part of the bay, is located the Midia Port, where between 1966 and 1971 a long extension of 5 km of the offshore was built. Because of this extension, the natural flow of sediments has been significantly changed. Thus, the southern part of the Mamaia Bay had less sand nourishment which meant that the coast was eroding and to prevent it a protection of six dikes was built. After approximately forty years of coastal erosion, the south of the Mamaia Bay had in 2016 a new protection scheme, which includes first of all the beach nourishment and a new dike structure (groins scheme for protection) to protect it. From this perspective, the objective of the proposed study is to evaluate the effectiveness of the old Master plan against the new one by modeling the outcome of the two scenarios and to perform a comparison with a third one, in which the protection dikes do not exist and only the artificial nourishment has been done. In order to assess the wave processes and the current patterns along the shoreline, a complex computational framework has been applied in the target area. This joins the SWAN spectral phase averaged model with the 1D surf model. Furthermore, new UAV technology was also used to map out, chart and validate the numerical model outputs within the target zone for a better evaluation of the trends expected in the shoreline dynamics.

Keywords: Black Sea; marine environment; wave regime; costal protection; shoreline changes

1. Introduction

The Black Sea, is an enclosed sea basin that can be considered the most distant extension of the oceans, since is linked through various straits via the Mediterranean Sea to the Atlantic Ocean. Despite the fact that it is not a very large sea, strong storms are often noticed in this area (see for example Rusu 2015, 2016). Such storms represent a real risk for the marine and coastal hazards (Gasparotti and Rusu 2012), but they may have also an unwished coastal impact. The most energetic part of the Black Sea is its western part (Rusu *et al.* 2016), whose coasts are subjected in this way to the most dynamic erosion processes (Rusu and Macuta 2008). Moreover, in this side of

*Corresponding author, Professor, E-mail: Eugen.Rusu@ugal.ro
[a] Ph.D. Student, E-mail: n.dragos8@gmail.com

 ISSN: 2093-6702 (Print), 2093-677X (Online)

the sea are located also the mouths of the Danube River, where the processes of wave-current interaction are very strong and these processes have a direct influence on the neighboring coastal dynamics (Ivan *et al.* 2012).

Nevertheless, the coasts are not influenced only by storms or other natural hazards, but they might be also influenced by various human activities or nearshore works. Thus, many coastal works that might appear at a first sight beneficial, prove to have on a medium to long term an unwished outcome. Such a case is discussed in the present work, which is focused on the Mamaia Bay (from the Romanian nearshore), in the western side of the Black Sea.

Fig. 1 The Black Sea basin in the summer season – Sentinel 2 (the red rectangle represents Mamaia Bay). Figure processed from Google Earth

Fig. 2 Mamaya Bay and the zone of interest. Figure processed from Google Earth

The coastal area considered in the present work (Mamaia beach), is a narrow stretch of sand barrier island that sits between Siutghiol Lake and the Black Sea. In the northern part of the bay, between the years 1966 – 1971, the Midia Port had built an extension to the offshore long of 5 km. Because of this extension the natural flow of sediment has been changed, and as a consequence the southern part of Mamaia Bay had less sand nourishment witch meant that the coast was eroding. In order to prevent it six dikes were built. Thus, it is expected that the coast will change in the future due to the new structures, as the current along the coast will change with it. As a result, after approximately forty years of coastal erosion the south of Mamaia Bay had in 2016 a new protection scheme, which includes first of all beach nourishment and a new dike structure (groins scheme for protection) to protect it, Omer *et al.* (2015).

From this perspective a complex system based on numerical models has been implemented in the target area considering the most relevant wave propagation patterns and three different scenarios. These scenarios concern the followings: a) the old configuration (the old Master Plan)-D-dikes only; b) the new configuration (the new Master Plan)-DN – dikes and nourishment; c) No dike protection, with nourishment only (a hypothetical situation). The study benefited also from a continuous survey of the target area by the new UAV technology that was also used to map out and chart the considered coastal sector, and further on to validate the numerical model outputs.

2. Methodolgy

2.1 Description of the experiment

The experiment was done in two steps. In the first part, the simulation was performed on a larger scale and in the second part the results of the first simulation were applied to a smaller scale using a nesting approach.

The bathymetry data considered in the simulation was acquired from the EMODnet website as a .xyz file. The shoreline GPS data was obtained /measured in the field before the nourishment and after it, respectively in 2015 and in the summer of 2016. The old dike system was mapped out from satellite images and the new dike system was mapped out using a UAV and specialized software to process the images (Agisoft PhotoScan).

The wind and wave parameters that were used as input for the SWAN model are the average wind and wave directions corresponding to the most relevant patterns. The main wave direction characteristic to Mamaia Bay is from E, with a frequency of 29%, followed by ENE, with 18%, this two directions alone make a sum of 47% for the wave distribution. Furthermore, for the present study the next two wave distributions were considered as well. These are NE and ESE (13% and 12%, respectively) to better simulate two different (almost opposite) situations, Niculescu *et al.* (2016) and Mateescu (2002).

ISSM (acronym from the Interface for SWAN and SURF models), Rusu *et al.* (2008), is a user friendly model system developed for a quick evaluation of the nearshore waves and currents. This is a computational framework that joins the SWAN spectral model with the 1D SURF model. SWAN (Simulating WAves Nearshore), Booij *et al.* (1999) is probably the most widely used wave model. Despite its range of applicability was further extended, the model was initially designed as a shallow water wave model and parameterization for some key physical processes in the nearshore, including a phase decoupled model for diffraction, are available.

Table 1 Characteristics of the computational domains defined for the SWAN model simulations and the physical parameterizations activated for large scale and high resolution simulations, respectively

SWAN	**Coordinates**	**Δx × Δy (m)**	**Δθ (°)**	**Δt (min)**	**nf**	**nθ**	***ngx* × *ngy* = *np***
Large scale	Cartesian	25 × 25	10	180 stat	34	36	299×591= 176609
High resolution	Cartesian	25 × 25	10	180 stat	34	36	154x239=36806

Input / Process	**Wave (m)**	**Wind (m/s)**	**Tide**	**Curr**	**Gen**	**Wcap**	**Quad**	**Triad**	**Diffr**	**Bfric**	**Set up**	**Br**
Large scale	X	X	0	0	X	X	X	X	X	X	0	X
High resolution	X	X	0	0	X	X	X	X	X	X	X	X

A simple, but a very effective model for the nearshore circulation is SURF, Mettlach *et al.* (2002), known also as the Navy Standard Surf Model. This is a parametric 1D model that estimates the wave induced longshore currents by solving only the longshore component of the momentum balance equation. Hence such a model can estimate only the longshore component of the nearshore currents, while a 3D model can also estimate the cross-shore component and the vertical variation of the currents. The justification for the existence of the 1D model is that longshore currents are most relevant in most of the coastal applications. This modelling system was considered in the present study, with the emphasis put on the wave modelling component.

Characteristics of the computational domains defined for the SWAN model simulations and the physical parameterizations activated for large scale and high resolution simulations, respectively. Δx and Δy represent the resolution in the geographical space, Δθ – resolution in directional space, Δt – time resolution, nf – number of frequencies in spectral space, nθ – number of directions in spectral space, ngx – number of grid points in x direction, ngy – number of grid points in y direction and np – total number of grid points. Wave – wave forcing, Tide – tide forcing, Wind – wind forcing, Curr – current field input, Gen – generation by wind. Wcap - whitecapping process, Quad – quadruplet nonlinear interactions, Triad – triad nonlinear interactions, Diff – diffraction, Bfric – bottom friction, Set up – wave induced set up, Br – depth induced wave breaking.

First of all, to get to the high resolution area of interest, where the three scenarios are considered, the input parameters for the small scale are needed. Thus, for the large scale model at the level of Mamaia Bay the input wave height value for the large scale model was 4 m, to simulate better the waves that can loose the sand from the shore for the current flow to move around and deposit it offshore.

As a consequence, to get the input parameters for the small scale model simulations, two large scale simulations were conducted (waves from NE and ESE), Vlasceanu *et al.* (2015). The main wind and wave parameters considered in the large scale the simulations are presented in Tables 1 and 2.

The second part of the study combined three situations, the old dike system, the new one with the sand nourishment and a third one in which only the sand nourishment has been done without any dikes.

Table 2 The two main wind directions and intensities considered in the large scale the simulations

	Wind storm parameters	
Direction	NNE – 22.5˚	SSE – 157.5˚
Speed	9 m/s	8 m/s

Table 3 The main wave parameters considered in the large scale the simulations

	Mean Wave parameters		Storm parameters	
Direction	NE – 45˚ - 13%	ESE – 112.5˚ - 12%	Direction	NE – 45˚ - 13%
HS	0.73	0.8	HS	0.73
T	3.6	4.7	T	3.6

2.2 Large scale simulations

The mean wave and wind parameters are not enough to change the coastline, as the wave energy that resides in a wave with the height of 0.8 m is too small. As such the wave height was changed to 4 m to simulate an actual storm that can cause the erosion process. The first two large scale simulation performed in the Mamaia Bay with the SWAN model are illustrated in Fig. 1 in terms of the wave vectors. The high resolution computational domain is indicated as well (Fig. 1(b)).

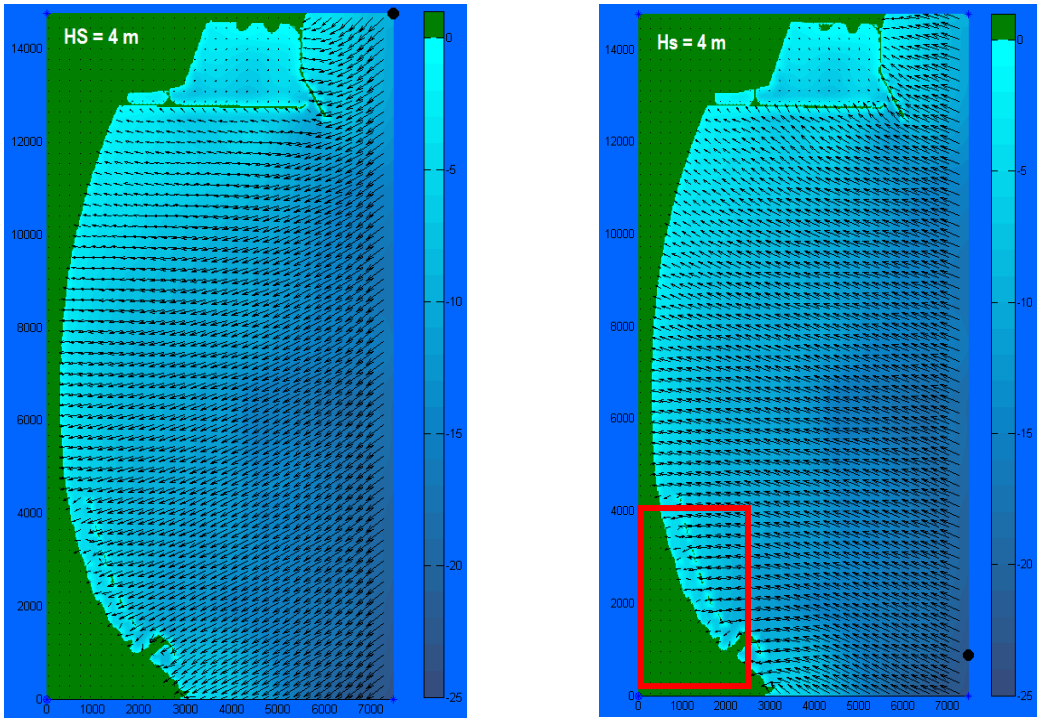

(a)Waves from NE (b)Waves from ESE

Fig. 3 First two large scale simulations (Mamaia Bay)

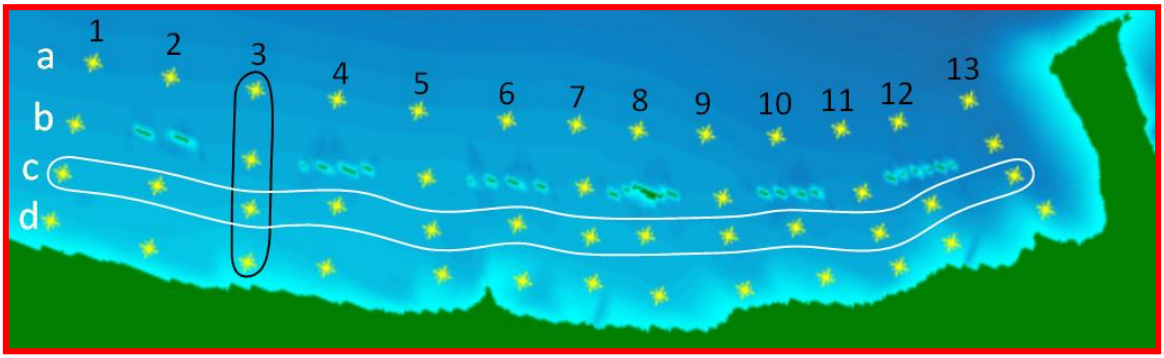

Fig. 4 Placement of all estimation points for the small scale situations (Dikes with nourishment)

2.3 High resolution simulations

The wave height and wave direction that resulted from the big scale simulation were used as input in the small scale (high resolution) simulations for the boundary condition. As expected the waves height and direction have changed because of the bathymetry, which rotates the wave direction through the process of refraction to be approximately normal to the shore.

There were chosen 46 points of interest to get the correspondingly wave heights for the three scenarios, representing 4(**a**, **b**, **c**, **d**) lines and 13 transects. The positions of these points are illustrated in Fig. 2, which displays also the identification of point **c** in transect **3.** It has to be mentioned that even the transects contain only 3 points (no **b** points) due to the dikes. While Fig. 2 presents the situation for the Dikes with nourishment, Fig. 3 present Dikes without nourishment scenario.

The bathymetric maps (Fig. 6) are made with the help of the Arc Map software. In the first scenario the dike system is renewed without the nourishment (this is an hypothetical situation were from any reason the nourishment wouldn't have taken place). The second scenario represents the real life situation with the nourishment and renewed dike system done. In the third scenario the dike system has been removed to show (by comparison with the other two scenarios) how much does the dike system influence the waves.

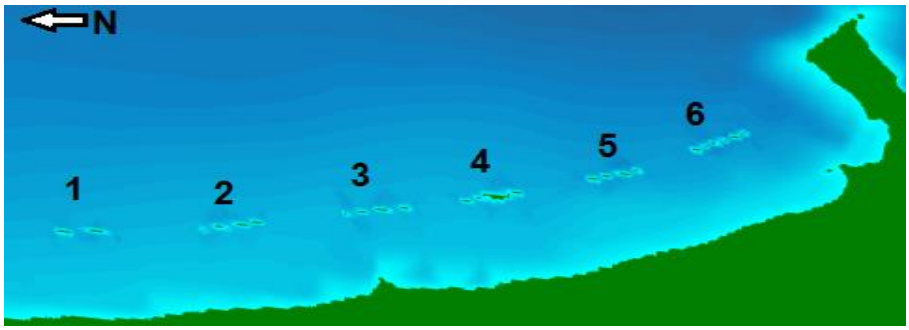

Fig. 5 Dikes without nourishment

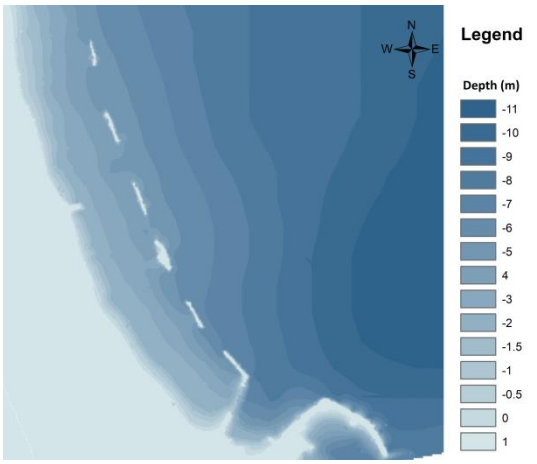

Scenario 1 (Dikes without nourishment)

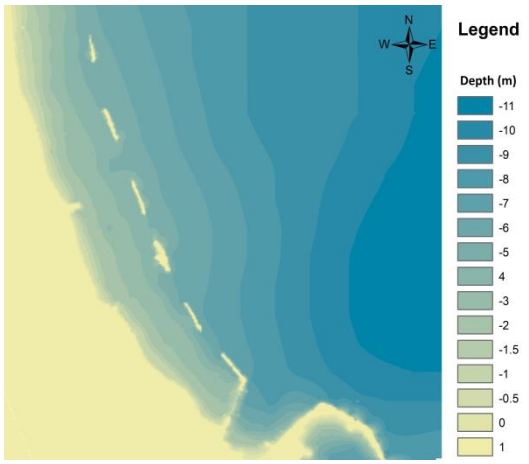

Scenario 2 (Dikes with nourishment)

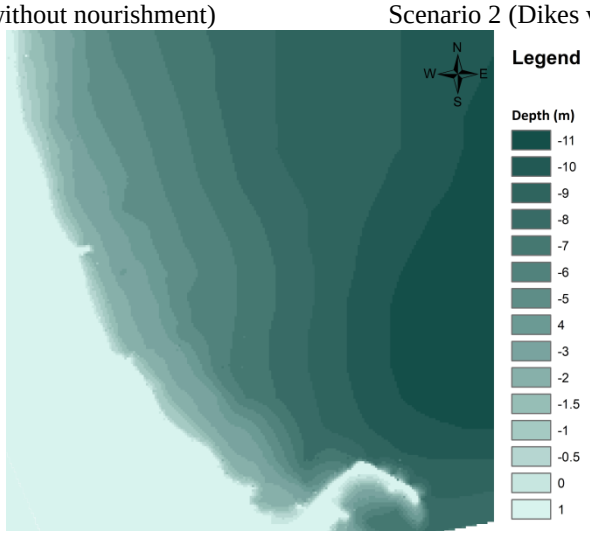

Scenario 3 (Nourishment without dikes)

Fig. 6 The bathymetry for the three scenarios

3. Results

Tables 3-5 given below allow comparing the wave heights in every estimation point for the three scenarios considered in the first case (NE waves and NNE wind)

3.1 Waves form NE and wind from NNE

The significant wave heights estimated for the points of main interest (**d** points close to the shore) are represented in Fig. 4. Each color of the significant wave heights represented in Fig. 4 indicates the situations provided in Tables 3-5, respectively, where the values highlighted are represented with the same color.

Table 4 Estimated wave heights for dikes without nourishment (D)

Transect	**1**	**2**	**3**	**4**	**5**	**6**	**7**	**8**	**9**	**10**	**11**	**12**	**13**
Point **a**	2.29	2.32	2.33	2.35	2.35	2.38	2.39	2.40	2.40	2.41	2.41	2.39	2.29
Point **b**	2.16		2.15		2.16		2.18		2.27		2.23		1.89
Point **c**	1.96	1.10	1.85	0.59	1.75	0.95	1.56	0.60	1.95	0.55	1.50	0.24	1.56
Point **d**	1.66	1.43	1.30	1.24	1.41	1.18	1.28	1.33	1.34	1.49	1.12	1.00	1.15

Table 5 Estimated wave heights for dikes with nourishment (DN)

Transect	**1**	**2**	**3**	**4**	**5**	**6**	**7**	**8**	**9**	**10**	**11**	**12**	**13**
Point **a**	2.29	2.32	2.33	2.35	2.35	2.38	2.39	2.40	2.40	2.40	2.41	2.39	2.29
Point **b**	2.16		2.15		2.16		2.18		2.27		2.23		1.89
Point **c**	1.96	1.10	1.85	0.59	1.75	0.95	1.56	0.60	1.95	0.55	1.50	0.24	1.56
Point **d**	1.66	1.43	1.30	1.24	1.41	1.18	1.28	1.33	1.35	1.49	1.12	0.99	1.12

Table 6 Estimated wave heights for no dikes with nourishment (N)

Transect	**1**	**2**	**3**	**4**	**5**	**6**	**7**	**8**	**9**	**10**	**11**	**12**	**13**
Point **a**	2.29	2.31	2.33	2.35	2.35	2.38	2.39	2.40	2.40	2.41	2.41	2.39	2.29
Point **b**	2.16		2.14		2.16		2.19		2.28		2.28		1.90
Point **c**	1.99	2.00	1.93	1.99	1.98	2.03	2.00	2.05	2.16	2.22	2.16	2.13	1.57
Point **d**	1.73	1.70	1.47	1.74	1.77	1.43	1.78	1.81	1.83	1.85	1.90	1.66	1.16

The significant differences of wave heights (at the shore, **d** points) in transects **2-12** occur only through the dikes existence (D-DN differences being irrelevant). There are no differences at the boundaries of the area because (**1**) the front touches the points without interacting with the dam, respectively (**13**), where the interaction with the southern external dike is major. Inside the area, both the values and the differences between D (or DN) and N are variables determined by dike-induced interferences and local bathymetry characteristics. Considering DN-N differences, the average difference is 0.38 m and the standard deviation is 0.22 m.

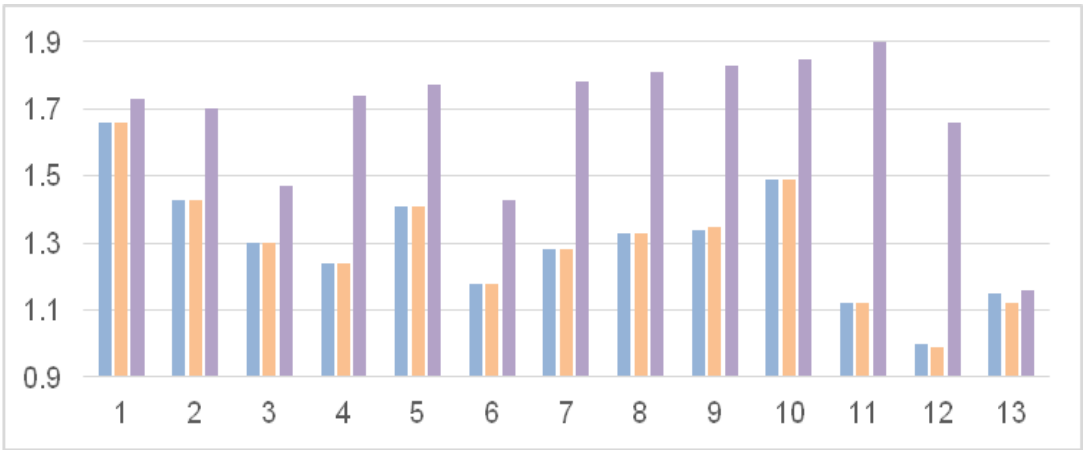

Fig. 7 Wave height difference between the three scenarios

3.2 Waves from ESE and wind from SSE

Tables 5-7 bellow allow comparing wave heights in every reference point for the three scenarios in the second case (SSE wind and ESE waves). The estimated wave heights for the points of main interest (**d** points close to the shore) are represented in Fig. 5. Each color of the significant wave heights represented in Fig. 5 indicates the situations provided in Tables 6-8, respectively, where the values highlighted are represented with the same color.

Table 7 Estimated wave heights for dikes without nourishment

Transect	**1**	**2**	**3**	**4**	**5**	**6**	**7**	**8**	**9**	**10**	**11**	**12**	**13**
Point **a**	2.58	2.56	2.56	2.56	2.56	2.56	2.55	2.55	2.55	2.54	2.50	2.37	2.20
Point **b**	2.35		2.31		2.30		2.23		2.32		2.10		1.67
Point **c**	2.03	1.31	1.85	0.90	1.56	1.13	1.22	0.85	1.74	0.69	1.09	0.27	1.25
Point **d**	1.70	1.58	1.28	1.49	1.12	1.33	1.12	1.54	1.05	1.55	0.73	1.08	0.85

Table 8 Estimated wave heights for dikes with nourishment

Transect	**1**	**2**	**3**	**4**	**5**	**6**	**7**	**8**	**9**	**10**	**11**	**12**	**13**
Point **a**	2.57	2.56	2.56	2.56	2.56	2.56	2.55	2.55	2.55	2.53	2.50	2.37	2.19
Point **b**	2.35		2.31		2.30		2.23		2.31		2.10		1.66
Point **c**	2.03	1.30	1.85	0.89	1.56	1.13	1.22	0.84	1.74	0.69	1.09	0.26	1.25
Point **d**	1.70	1.58	1.28	1.49	1.12	1.33	1.12	1.53	1.05	1.55	0.73	1.07	0.84

Table 9 Estimated wave heights no dikes with nourishment

Transect	**1**	**2**	**3**	**4**	**5**	**6**	**7**	**8**	**9**	**10**	**11**	**12**	**13**
Point **a**	2.58	2.56	2.56	2.56	2.56	2.56	2.55	2.55	2.55	2.54	2.50	2.37	2.20
Point **b**	2.36		2.30		2.31		2.31		2.36		2.23		1.67
Point **c**	2.12	2.13	2.04	2.11	2.10	2.14	2.10	2.15	2.19	2.23	2.05	1.96	1.26
Point **d**	1.80	1.76	1.48	1.82	1.83	1.50	1.85	1.85	1.83	1.86	1.80	1.55	0.86

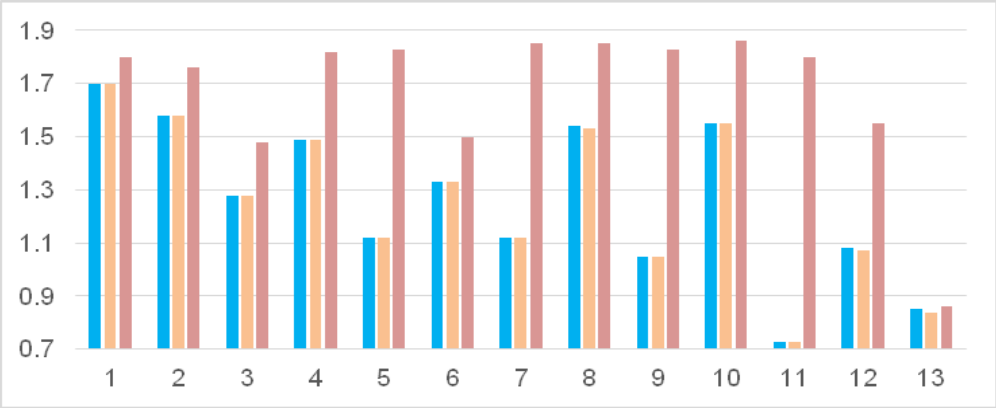

Fig. 8 Wave height difference between the three scenarios - waves from ESE

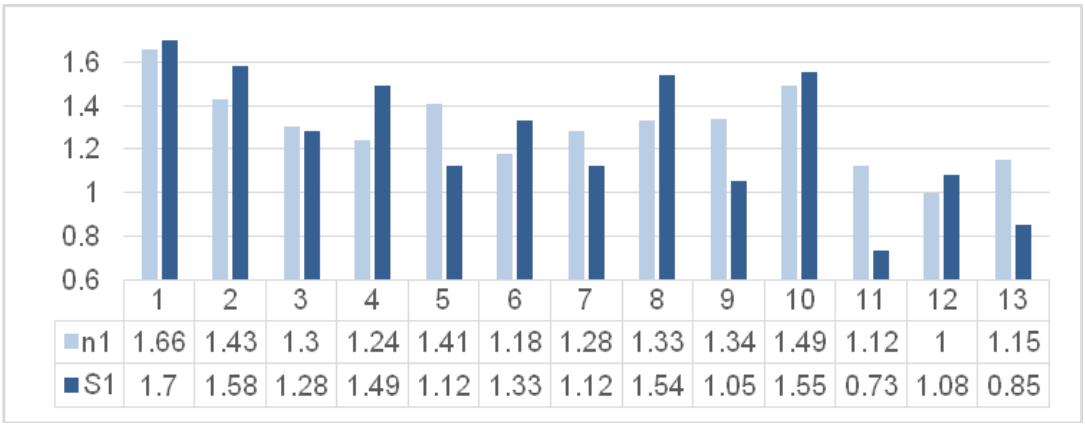

	1	2	3	4	5	6	7	8	9	10	11	12	13
n1	1.66	1.43	1.3	1.24	1.41	1.18	1.28	1.33	1.34	1.49	1.12	1	1.15
S1	1.7	1.58	1.28	1.49	1.12	1.33	1.12	1.54	1.05	1.55	0.73	1.08	0.85

Fig. 9 Wave height difference between wave directions – scenario 1

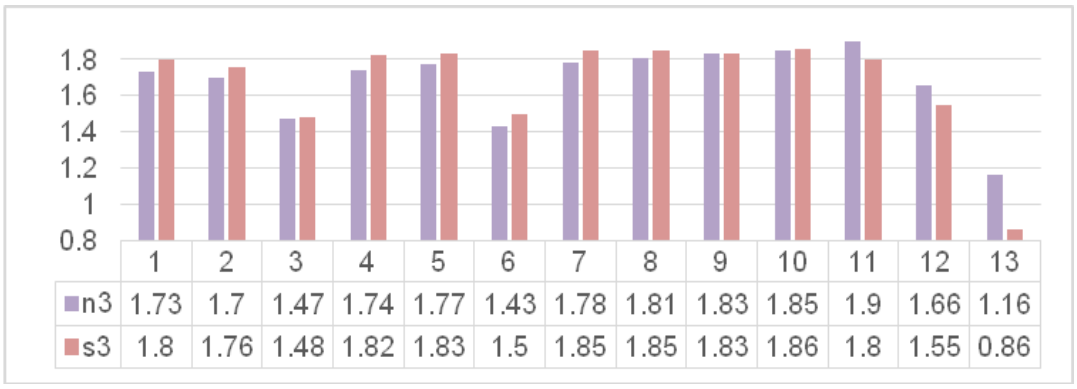

	1	2	3	4	5	6	7	8	9	10	11	12	13
n3	1.73	1.7	1.47	1.74	1.77	1.43	1.78	1.81	1.83	1.85	1.9	1.66	1.16
s3	1.8	1.76	1.48	1.82	1.83	1.5	1.85	1.85	1.83	1.86	1.8	1.55	0.86

Fig. 10 Wave height difference between wave directions – scenario 3

Through comparison, the differences between D-DN (Fig. 6) remain irrelevant. The variability of the differences is higher (transects **4** to **12**) due to the interference asymmetries that appear from the southern dike. Indeed, for the whole set the differences average is 0.42 m and the standard deviation is 0.32 m.

In the case (presented in Fig. 6) where the dikes exist (scenario 1), the differences between the wave velocities determined by the wave direction NE(n1) or SE(S1), the spread of values (0.65 m) is relatively high (0.25 ÷ -0.4) m; the average for all is 0.04 m with a standard deviation of 0.22 m. The determining factors are the interference phenomena and the bathymetry.

In the absence of dikes (scenario 3, Fig. 7), the spreading of the values (0.37 m) of the differences (between the wave heights) determined by the direction of the waves (NE or SE) is relatively small (-0.3 ÷ 0.07) m, for the whole set, the average being 0 m and the standard deviation 0.11 m. The determination is mostly due to the bathymetry.

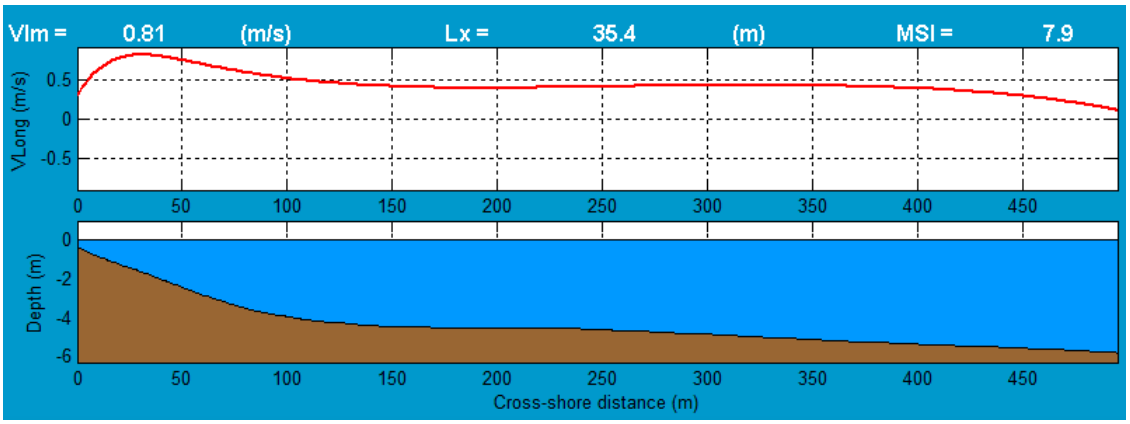

Fig. 11 Profile no. 1 (current velocity along depth)

Table 11 Maximum current velocities along the shore (m/s) – waves from NE

	Situations		
Current profiles	D	DN	N
P1	0.81	0.94	0.79
P2	0.83	1.4	0.84
P3	0.76	0.83	1.08
P4	1.3	0.85	

In Fig. 8, the red line (first graph) represents the current that runs along the shore and how it varies across the profile with depth. The major variation is noticed in the first 100 m, where the current velocity fluctuates from -0.29 to -0.81 (meaning that it runs southward). Due to the fact that in Fig. 9 all the profiles had to be joined together to better show the results and how they are connected, the profiles are not that readable, and so for a clearer view, profile no. 1 is enlarged (Fig. 8). The maximum current velocities along the shore (m/s) for the case when the waves are coming from NE are given in Table 10.

For the Scenario D, it is estimated that the maximum speed along the shore is estimated to be from N to S at an increasing distance from shore 30 m, 30 m, 70 m, 125 m (P1, P2, P3, P4). The speed drops slightly (P1, P2, P3) but on profile P4 it is ~ 50% higher.

For DN Scenario, the maximum speed along the shore is generally 30-40 m (except P3 where the maximum of 0.8 m /s is at 330 m offshore due to the bathymetric profile, the second maximum of 0.6 m/s being still at 30 m). The speeds (P1, P3, P4) are close except for profile P2 (where it is higher by ~ 50%).

Below, there are illustrated the current and bathymetric profiles results for each scenario (D, DN and N) with waves from NE, Hs 4, T 6.5, and wind from NNE, 9 m/s.

The current profiles and the corresponding significant wave heights from (waves ESE, Hs 4, T 6.5, wind from SSE, 8 m/s) are illustrated in Fig. 12 while Table 13 presents the maximum current velocities along the shore (m/s) – waves from SE

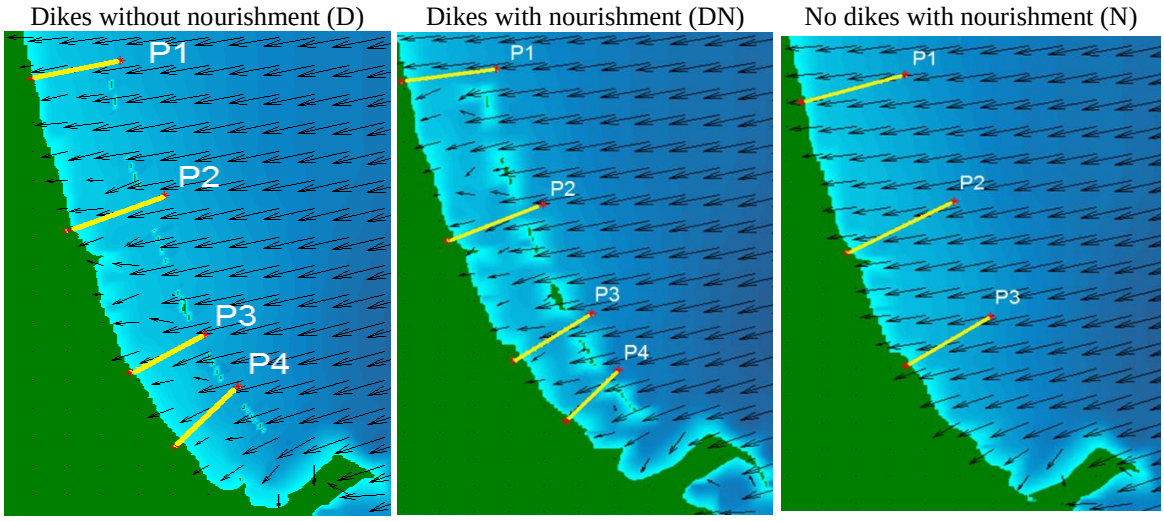

Fig. 12 Profile layout and wave simulation for the three situations (waves from NE, Hs 4, T 6.5, and wind from NNE, 9 m/s)

In the absence of dikes (scenario N) the maximum speed along the shore is generally 25-35 m from the shore, the speed at the last profile being higher by ~ 25%. In the above mentioned case the currents are obviously negative (towards N).

For scenario D, it is observed that the maximum speed along the shore is estimated to be observed from N to S at an increasing distance from the shore 30 m, 25 m, 75 m, 100 m (P1, P2, P3, P4). The speed drops to the South (P1, P2, P3), but for the profile P4 it is ~ 50% higher than the average of the other three. A further 2D or 3D modeling of the currents would probably explain the phenomenon.

For DN Scenarios, the currents across the profile are generally lower. The maximum speeds are ~ 30 m from the shore (P1, P2, P3) with the exception of the profile P4, where it is at 250 m, the second maximum being also 30 m from the shore. Similar to the scenario D, high speeds are recorded at the ends (Profiles 1 and 4). Scenario N shows a higher current in the northern part (profile 1).

Profile No. Current and bathymetric profiles

1

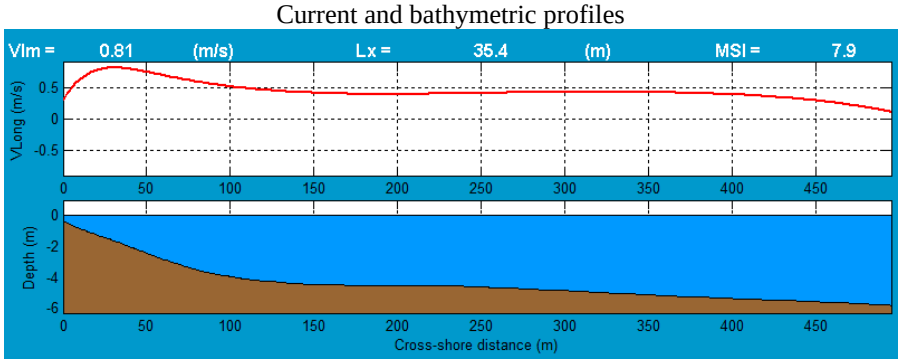

Continued-

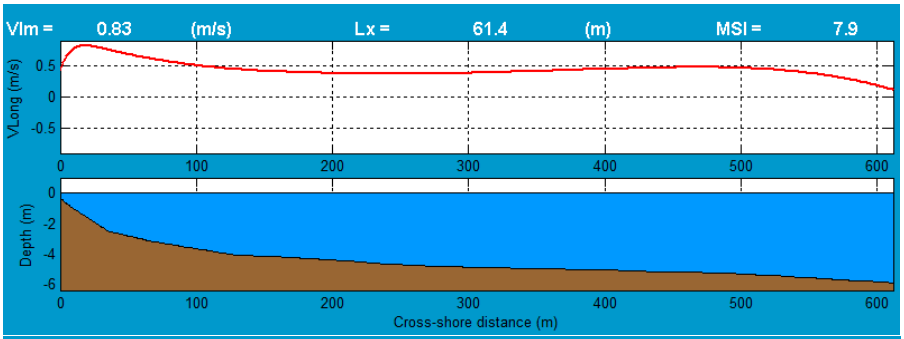

2

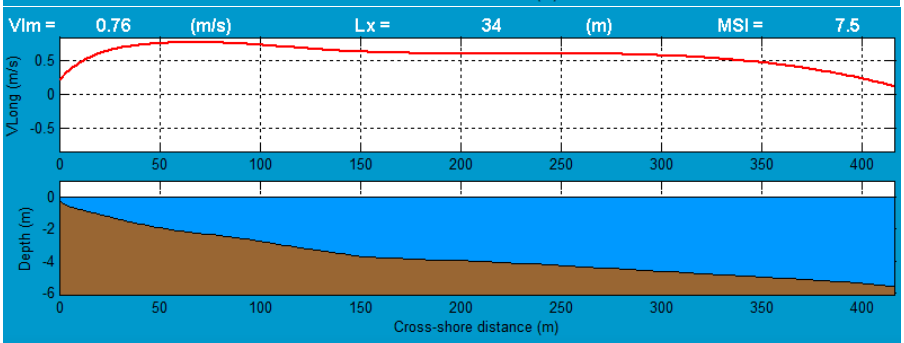

3

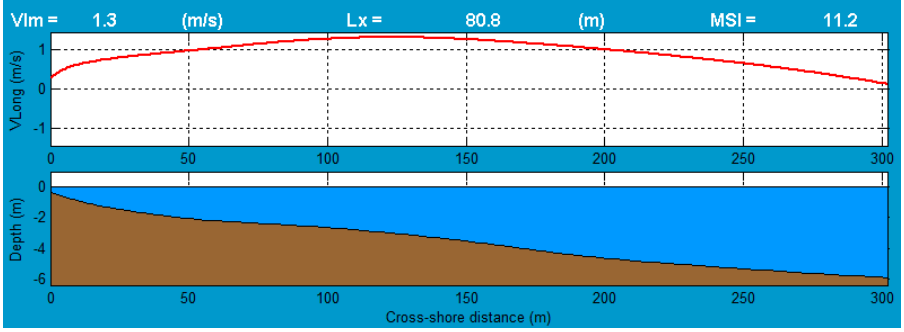

4

(a)

Profile No. Current and bathymetric profiles

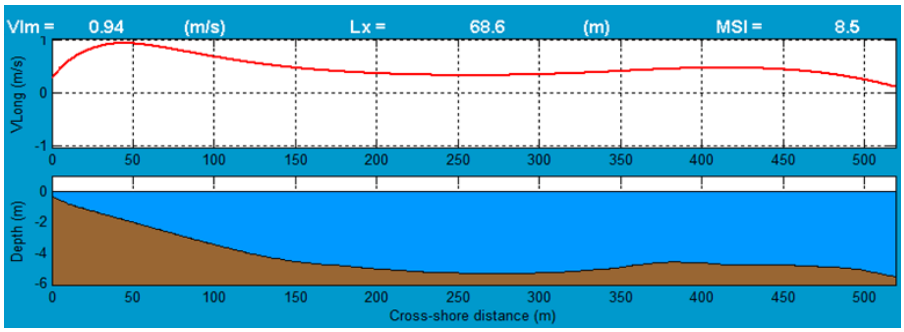

1

Continued-

2

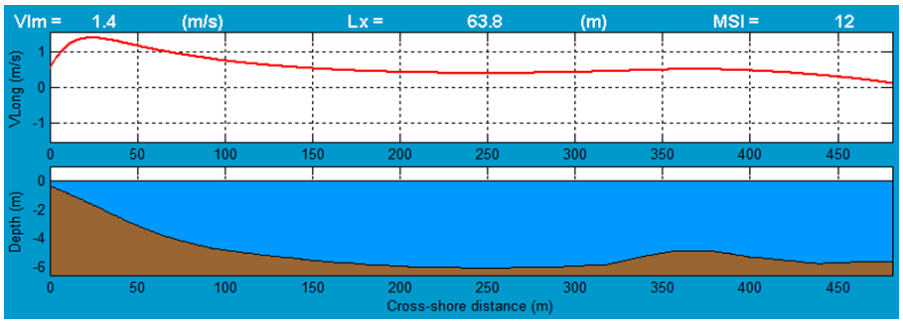

3

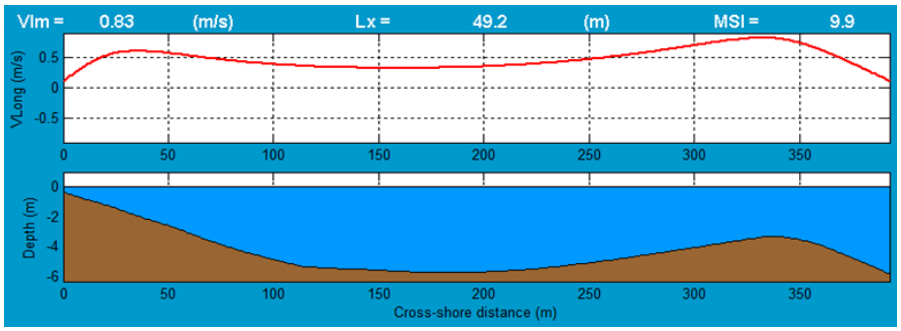

4

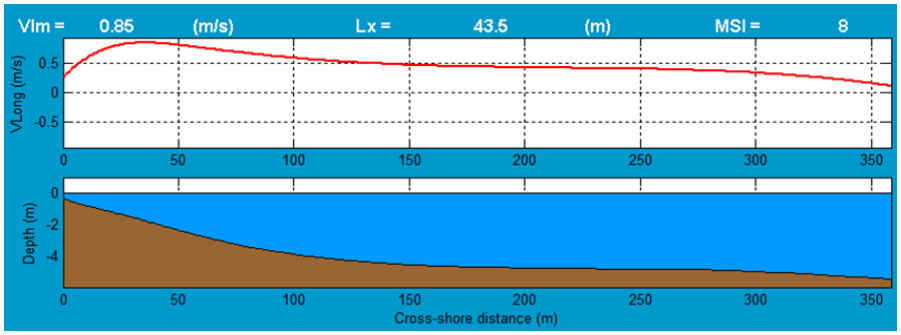

(b)

Profile No. Current and bathymetric profiles

1

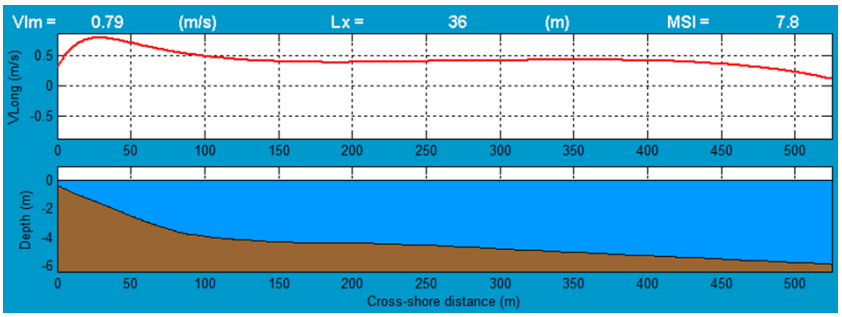

Continued-

2

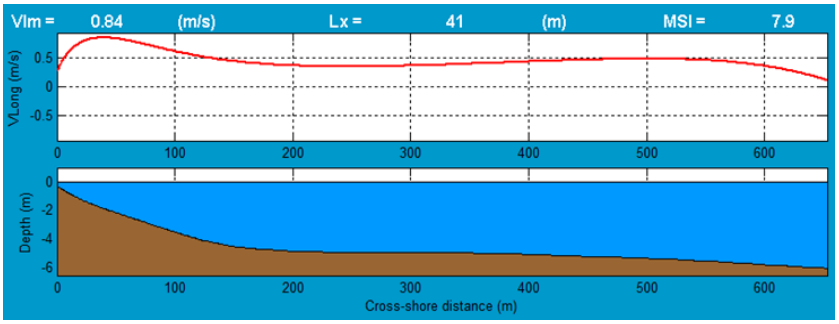

3

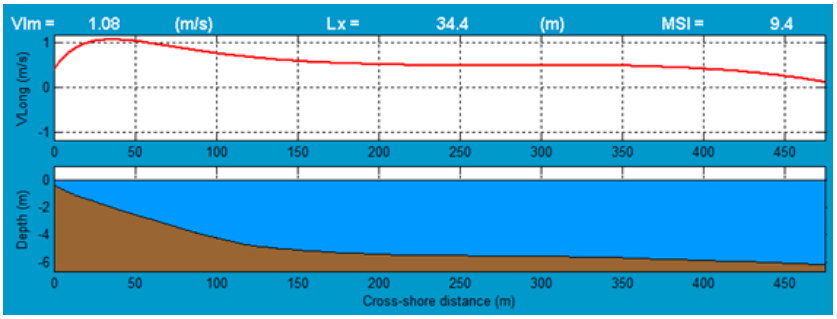

(c)

Fig. 12 (a) Current and bathymetric profiles for the first situation (D), (b) Current and bathymetric profiles for the second situation (DN) and (c) Current and bathymetric profiles for the third situation (N)

Dikes without nourishment (D) Dikes with nourishment (DN) No dikes with nourishment (N)

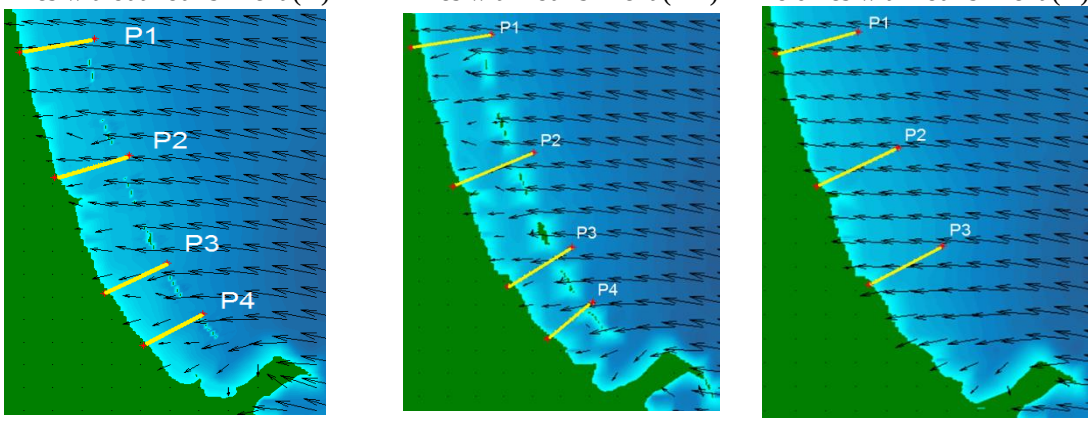

Fig. 13 Profile layout and wave simulation for the three situations(waves ESE, Hs 4, T 6.5, wind from SSE, 8 m/s)

Below (in Figs. 14(a)-14(c)) are the current and bathymetric profiles results for each scenario (D, DN and N) with waves from ESE, Hs 4, T 6.5, wind from SSE, 8 m/s.

Profile No. Current and bathymetric profiles

1

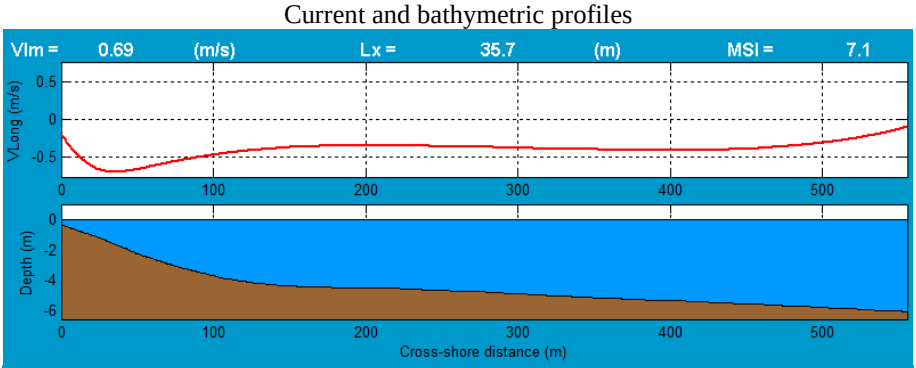

2

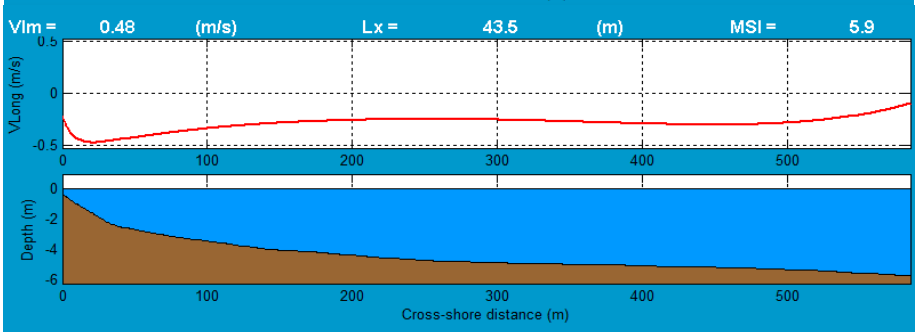

3

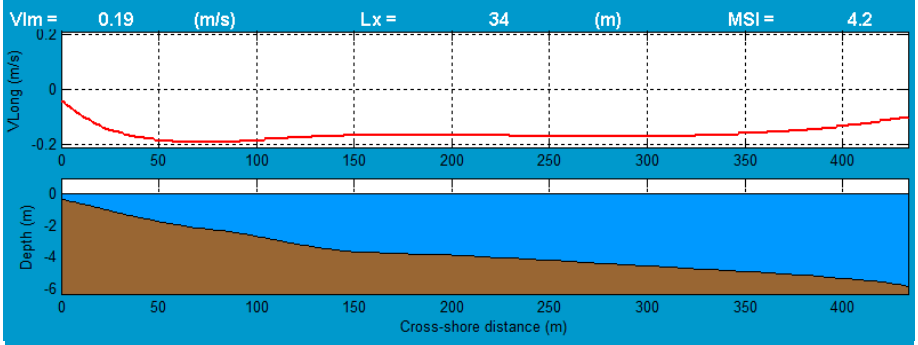

4

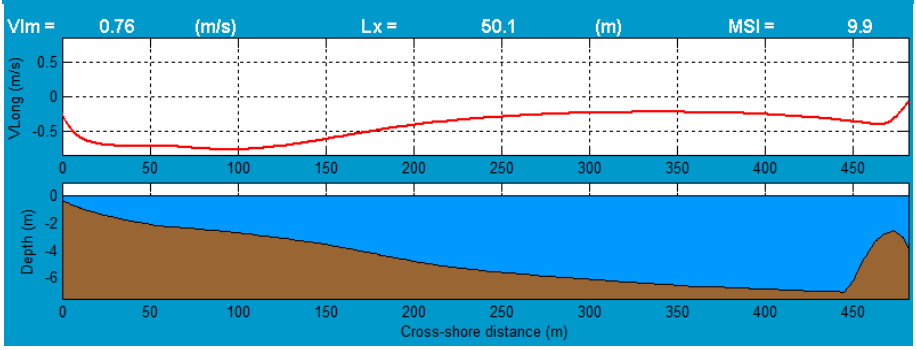

(a)

Continued-

Profile No.	Current and bathymetric profiles
1	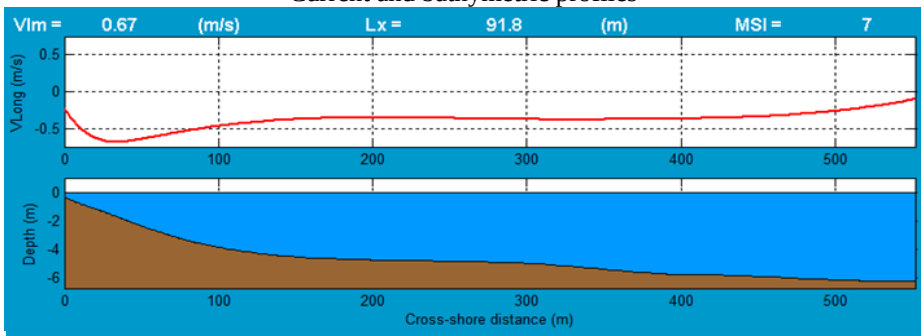
2	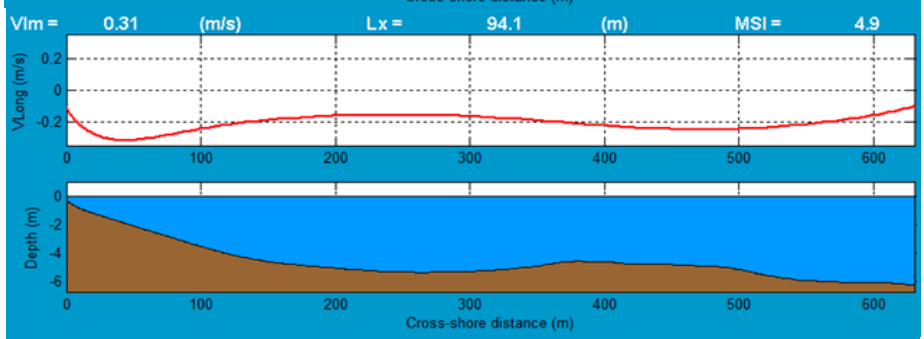
3	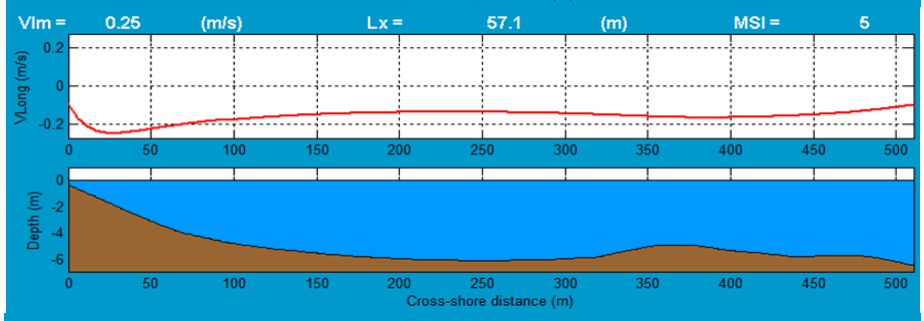
4	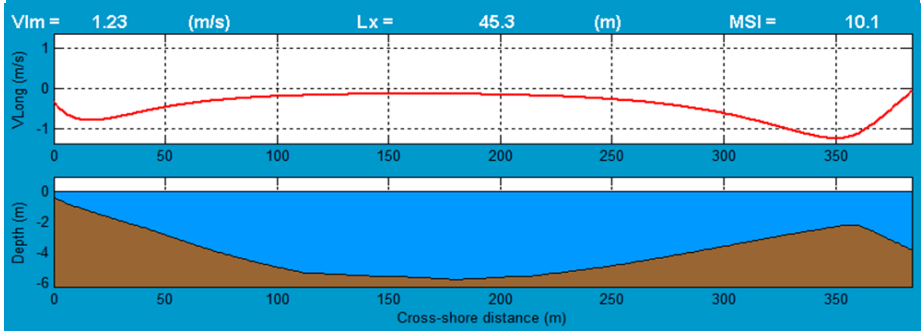

(b)

Continued-

Profile No. Current and bathymetric profiles

1

2

3

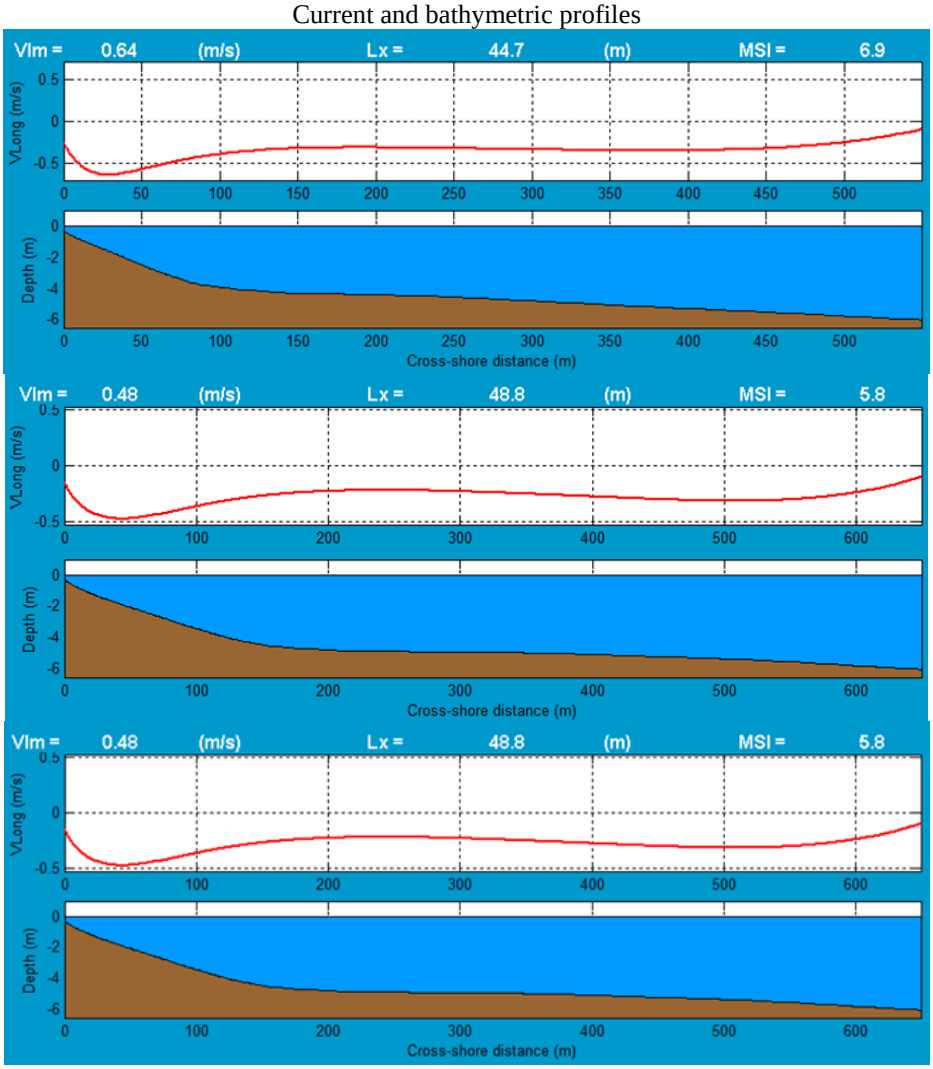

(c)

Fig. 14 (a) Current and bathymetric profiles for the first situation (D), (b) Current and bathymetric profiles for the first situation (DN) and (c) Current and bathymetric profiles for the first situation (N)

Table 13 Maximum current velocities along the shore (m/s) – waves from SE

	Situations		
Current profiles	D	DN	N
1	-0.69	-0.67	-0.64
2	-0.48	-0.31	-0.48
3	-0.19	-0.25	-0.48
4	-0.76	-1.23	

Finally, it has to be also highlighted that the results of the modeling system have been validated for each relevant propagation pattern by means of the new UAV technology that was constantly used to survey the target area.

5. Conclusions

The approach presented in this work highlights the complexity of the phenomena occurring near the shore, especially in the case of bad weather conditions; the influence of the wave height distribution and of the nearshore current velocity (driving the sediment transport), will cause changes in the bathymetry that will alter the area's response to the next storms.

Although no in-depth analysis has been carried out, the variability found between the three scenarios occurs as evident (even if the wave heights of the D and DN scenarios are very close). Increasing the protection efficiency through sand nourishment seems relatively small.

Nevertheless, at this point the next issues must be also taken into consideration:

- The change in the stability of the beach, caused by the nourishment and its conseq uences in time;
- The consequences in time on the rearranging of sediments;
- Possible major predictable changes in extreme weather situations.

Estimation of possible changes should be improved by analyzing the distribution of the currents in areas of high water agitation and determining the divergence zones (where the probability of deposition increases). In this way, it is possible to forecast the temporal evolution of the bathymetry of the area and of the shoreline.

The authors propose the development of these analyzes in time, as the area (Mamaia bay) is of great socioeconomic importance, and includes specific situations that may apply to other areas of interest, Cristescu *et al.* (2016).

Finally, it can be also highlighted that the studies related the improvement of the coastal protection are still ongoing. Among various methods, the effect of the marine energy farms, besides delivering energy, represent also an alternative solution for the coastal protection. From this perspective, the studies developed by Rusu (2016), Zanopol *et al.* (2014a, b) and Diaconu and Rusu (2013) in the same nearshore targeted by the present work (or very close to it) showed that the presence of such marine farms may play a very dynamic role in the coastal protection. Thus, although the Black Sea cannot be considered very attractive from the perspective of the wave energy extraction, the wind energy is quite significant (see for example Onea *et al.* 2015, Onea and Rusu 2016) and together with the development of the wave energy extraction technologies, and especially those dedicated to the small amplitude waves, the hybrid wind-wave solutions might become viable in such coastal environments.

Acknowledgments

This work was carried out in the framework of the research project REMARC (Renewable Energy extraction in MARine environment and its Coastal impact), grant number PN-III-P4-IDPCE-2016-0017, financed by the Romanian Executive Agency for Higher Education, Research, Development and Innovation Funding – UEFISCDI.

References

Booij, N., Ris, R.C. and Holthuijsen, L.H. (1999), "A third generation wave model for coastal regions. Part 1: Model description and validation", *J. Geophys. Res.*, **104C4**, 7649-7666.

Cristescu, T.M., Ganea, G., Niculescu, A., Buga, L., Nedelcu, M., Diaconeasa, D., Mateescu, R. and Niculescu, D. *(*2016), "Wind data analysis for NIMRD's oceanographic measurement point 'estacada Mamaia' ", *Cercetari Marine*, **46**(4), 19-30.

Diaconu, S. and Rusu, E. (2013), The environmental impact of a Wave Dragon array operating in the Black Sea, *The Scientific World Journal*, ID 498013.

Niculescu, D. and Rusu, E. (2016), "Study of the wind regime in the north western part of the Black sea", *Mechanical Testing and Diagnosis*, **2**, 25-34.

Gasparotti, C. and Rusu, E. (2012), "Methods for the risk assessment in maritime transportation in the Black Sea basin", *J. Environ. Protection Ecology*, **13(**3), 1751-1759.

Ivan, A., Gasparotti, C. and Rusu, E. (2012), "Influence of the interactions between waves and currents on the navigation at the entrance of the danube delta", *J. Environ.Protection Ecology*, **13**, 1673-1682.

Mettlach, T.R., Earle, M.D. and Hsu, Y.L. (2002), "Software design document for the navy standard surf model, version 3.2", *Rep. Prepared for Naval Research Laboratory*, Stennis Space Center, Miss.

Onea, F.; Raileanu, A. and Rusu, E. (2015), "Evaluation of the Wind Energy Potential in the Coastal Environment of Two Enclosed Seas", *Adv. Meteorology*, ID 808617.

Onea, F. and Rusu, E. (2016), "Efficiency assessments for some state of the art wind turbines in the coastal environments of the Black and the Caspian seas", *Energy Exploration & Exploitation*, **34**(2), 217-234.

Omer, I., Mateescu, R., Rusu, L., Niculescu, D. and Vlăsceanu, E. (2015), "Coastal works extensions on the Romanian tourists littoral, its ecological impacts on the nature bathing areas", *J. Environ. Protection Ecology*, **16**(2), 417-424.

Mateescu, R. (2002), *The reconsideration of protection engineering solutions implemented to Mamaia beach Ovidius University Annals of Constructuion*, **1**(3-4), 423-439.

Rusu, E. and Măcuță, S. (2009), "Numerical modelling of longshore currents in marine environment", *Environ. Eng. Management J.*, **8**(1), 147-151.

Rusu, E., Conley, D.C. and Coelho, E. F. (2008), "A hybrid framework for predicting waves and longshore currents", *J. Mar. Syst.*, **69**, 59-73.

Rusu, E. (2014), "Evaluation of the wave energy conversion efficiency in various coastal environments", *Energies*, **7**, 4002-4018.

Rusu, E. (2016), "Analysis of the effect of a marine energy farm to protect a biosphere reserve", *MATEC Web of Conferences*, **62**, EDP Sciences.

Rusu, L., Butunoiu, D. and Rusu, E. (2014), "Analysis of the extreme storm events in the Black Sea considering the results of a ten-year wave hindcast", *J. Environ.Protection Ecology*, **15**(2), 445-454.

Rusu, L. (2015), "Assessment of the wave energy in the Black Sea based on a 15-year hindcast with data assimilation", *Energies*, **8**(9), 10370-10388.

Vlasceanu, E., Niculescu, D., Omer I. Rusu, E. and Ivan, A. (2015), "Offshore wave regime investigations towards safety port operations in the transitional zone of the Romanian coast", *Proceedings of the 15th International Multidisciplinary Scientific GeoConference SGEM 2015*, Book 3, vol 2, 675-682, Albena, Bulgaria, June.

Zanopol, A.T., Onea, F. and Rusu, E. (2014a), "Coastal impact assessment of a generic wave farm operating on the Romanian nearshore", *Energy*, **72**, 652-670.

Zanopol, A.T., Onea, F. and Rusu, E. (2014b), "Evaluation of the coastal influence of a generic wave farm operating in the Romanian nearshore", *J. Environ. Protection Ecology*, **15**, 597-605.